ROBOTIC MANIPULATION OF A HYPER-FLEXIBLE BODY

Hiromi Mochiyama * **Hideo Fujimoto** **

* *Touch Technology Laboratory funded by TOYOTA, Nagoya Institute of Technology, Faculty of Engineering, Gokiso-cho, Showa-ku, Nagoya 466-8555, Japan.*
** *Robotics and Automation Laboratory, Nagoya Institute of Technology, Faculty of Engineering, Gokiso-cho, Showa-ku, Nagoya 466-8555, Japan.*

Abstract: A hyper-flexible body is a continuum mechanical object with infinitely many kinematic degrees of freedom which can not be appropriately modeled as elastic bodies nor fluid. In this paper, manipulation of a hyper-flexible body is considered. Although we have only a few control input for the infinite-dimensional system of a hyper-flexible body, we provide an illustrative control example where we can achieve damping injection to a planar cable-like hyper-flexible body by only translational acceleration input at its one end. The control law is derived by the passivity approach based on the port-controlled Hamiltonian system representation.

Keywords: Robotics, Robot kinematics, Robot dynamics, Robot control, Flexible arms, Distributed parameter systems, Nonlinear systems, Mechanical systems

1. INTRODUCTION

A hyper-flexible body (An HFB, for short) is a continuum mechanical object with infinitely many kinematic degrees of freedom which can not be appropriately modeled as elastic bodies nor fluid. We can easily find this category of objects around us. Examples include clothes such as a jacket, a handkerchief and a necktie; papers such as a newspaper and a copy paper; leathers such as a bag and a glove; and plastic, foods, plants and so on. Considering manipulation of HFBs, we have to note the following properties of HFBs as controlled systems:

- The number of kinematic degrees of freedom of an HFB is *infinite* essentially. Moreover, an HFB is not necessarily modeled as a linear system, because we often have a wide ranges of displacement at each kinematic degrees of freedom. Its *nonlinear* nature should be considered.
- As a matter of practice, it is impossible to actuate all the degrees of freedom independently and simultaneously, which means an HFB is properly modeled as a *hyper-underactuated* system.
- As a matter of practice, it is impossible to obtain the sensory information about all the degrees of freedom independently and simultaneously, which means an HFB is the system of *highly-limited-sensing*.

Taking the above properties of HFBs into account, it seems hopeless to manipulate the system. It is, however, worth noticing that humans can manipulate such an object dexterously, where we can see the possibility to build up a useful theory for HFB systems.

The purposes of this research are (1) to find useful applications of systems with hyper-flexible bodies, and (2) to establish a useful manipulation theory of hyper-flexible bodies.

To achieve the goals above, we first try to find successful control examples of hyper-flexible systems, and then extract some essentials of the systems from phenomena of those examples.

It is reasonable to categorize hyper-flexible systems into the following classes based on the topological structure in three-dimensional Euclidean space:

- One-dimensional Structure: strings, cords, cables, limbs and trunks of vertebrates
- Two-dimensional Structure: clothes, papers, nets, human hands
- Three-dimensional Structure: food such as dough, clay, skins

We regard the class of one-dimensional structure as the most important class of hyper-flexible systems to be analyzed from the following reasons:

- The kinematic equations of hyper-flexible systems with one-dimensional structure can be expressed by Frenet-Serret formula of a spatial curve which represents the geometric feature of a curve simply (Kobayashi, 1995). This enables us to interpret the meanings of various related values and equations geometrically.
- The exact continuum dynamic equations of hyper-flexible bodies with one-dimensional structure are available. The dynamic equations are derived from those of a serial-rigid chain by the limit operation that the number of its degrees of freedom goes to infinity (Mochiyama and Suzuki, 2003*a*). Thus, we can discuss control problems based on its exact dynamics.
- There are some interesting manipulation examples of hyper-flexible systems in this one-dimensional structure, such as casting in fishing and top whipping.

We can find some related researches about manipulation of a cable-like hyper-flexible body with one dimensional structure.

Arisumi et al. proposed an excellent idea of casting manipulation inspired by casting in fishing (Arisumi *et al.*, 1999). This casting manipulation is the pioneering example of manipulation of hyper-flexible bodies. Ichikawa and Hashimoto regarded a cable as a planar serial-rigid chain, and verified the effectiveness of their identification and position control methods by experiments (Ichikawa and Hashimoto, 2001). Wakamatsu et al. proposed a planning method for knotting or raveling manipulation of cable-like objects (Wakamatsu *et al.*, 2004).

In our research, we take the exact continuum nature of the kinematics and dynamics of hyper-flexible bodies into account, which is clearly different point from the above related researches in the past. This continuum treatment of hyper-flexible bodies allows us to see physical and geometric handling of values and equations appeared in control problems. We will see this later in this paper.

In this paper, damping control of a planar cable-like hyper-flexible body is considered. In section 2, we show the kinematics and dynamics of a planar cable. In section 3, a damping control law is derived base on the passivity consideration by using the port-controlled Hamiltonian system representation. In section 4, the effectiveness of the derived control law is verified by a numerical simulation of a serial-rigid chain with 50 degrees of freedom. In section 5, we summarize the results of this paper.

2. PLANAR MOTION OF CABLES

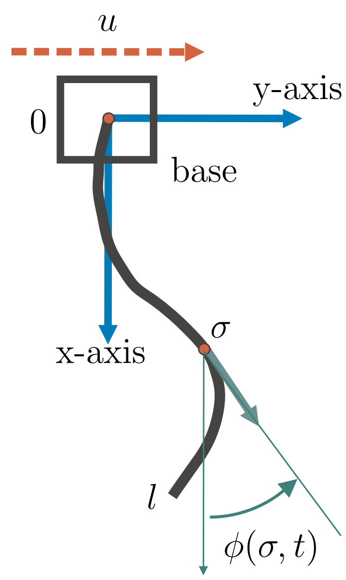

Fig. 1. Planar cable-like hyper-flexible body

In this paper, only the planar kinematics and dynamics of a cable-like hyper-flexible bodies are considered. More general models such as 3D case can be found in (Mochiyama and Suzuki, 2003*a*)

2.1 Geometry and Kinematics

Let $\theta(\sigma, t) \in \Re$ denotes the curvature of the backbone curve which characterizes the shape of a cable-like hyper-flexible body, where $\sigma \in [0\ l]$ and $t \in [0\ \infty)$ mean the arc length and the time respectively. The constant l is the total length of the object. The one end of the object is fixed at the base body, and the other end is free. Suppose that we can move the base body in the horizontal direction, and exert an acceleration $u \in \Re$ as a control input to this base body. The direction of the gravitational acceleration is in the direction of the x-axis of the coordinate frame attached at the base body. The gravitational acceleration constant is represented by g. Let $\phi(\sigma, t) \in \Re$ be the angle between the tangent of the shape curve at σ and the x-axis. Note that $\phi(\sigma, t) = \int_0^\sigma \theta(\eta, t) d\eta$.

In this research, we regard a one-dimensional hyper-flexible body as a continuous chain of slices with an infinitesimal width perpendicular to the backbone curve. Let $m(\sigma)$ and $I(\sigma)$ be a mass and inertia moment density around the z-axis of a slice at σ respectively. We assume that the center of mass of the slice is on the backbone curve. This is reasonable assumption for homogeneous and thin ropes.

2.2 Lagrange Dynamics

The dynamics of a hyper-flexible body with one-dimensional structure moving in a plane can be expressed by

$$\int_0^l \mathcal{M}(\sigma, \eta, t)\theta_{tt}(\eta, t) d\eta + \int_0^l \mathcal{C}(\sigma, \eta, t)\theta_t(\eta, t) d\eta + \mathcal{G}(\sigma, t) = \mathcal{U}(\sigma, t), \quad (\sigma \in [0\ l]) \quad (1)$$

where subscripts t and tt stand for the 1st and 2nd order partial derivatives with respect to the time respectively (Mochiyama and Suzuki, 2003*a*). The values $\mathcal{M}(\sigma, \eta, t) \in \Re$, $\mathcal{C}(\sigma, \eta, t) \in \Re$, $\mathcal{G}(\sigma, t) \in \Re$ and $\mathcal{U}(\sigma, t) \in \Re$ are, respectively, the counterparts of the row vectors of the inertial matrix and the Coriolis matrix, the elements of the gravitational torque vector, and the external torque appeared in serial-rigid chain dynamics. These values are defined as follows:

$$\mathcal{M}(\sigma, \eta, t) := \tilde{I}(\max(\sigma, \eta)) + \int_\eta^l \int_\sigma^l \tilde{m}(\max(\iota, \xi)) \cos {}^\iota\phi(\xi, t) d\iota d\xi \quad (2)$$

$$\mathcal{C}(\sigma, \eta, t) := \int_0^l \Gamma(\sigma, \eta, \nu, t)\theta_t(\nu, t) d\nu \quad (3)$$

$$\mathcal{G}(\sigma, t) := \int_\sigma^l \tilde{m}(\eta) \sin \phi(\eta, t) d\eta \ g \quad (4)$$

$$\mathcal{U}(\sigma, t) := \int_\sigma^l \tilde{m}(\eta) \cos \phi(\eta, t) d\eta \ u \quad (5)$$

where ${}^\iota\phi(\xi, t) := \phi(\xi, t) - \phi(\iota, t)$, $\tilde{I}(\sigma) := \int_\sigma^l I(\xi) d\xi$ and $\tilde{m}(\sigma) := \int_\sigma^l m(\eta) d\eta$. Moreover, $\Gamma(\sigma, \eta, \nu, t) \in \Re$ is defined by

$$\Gamma(\sigma, \eta, \nu, t) = - \int_{\max(\eta,\nu)}^l \int_\sigma^l \tilde{m}(\max(\iota, \xi)) \sin {}^\iota\phi(\xi, t) d\iota d\xi \ . \quad (6)$$

Note that the system represented by (1) is infinite-dimensional because the curve parameter σ continuously takes the value from 0 to l along the backbone curve. Moreover, the system described above is hyper-underactuated because we have only one input u in $\mathcal{U}(\sigma, t)$ in spite of the infinite dimensionality of the system. In this paper, we ignore the position of the base body which is obtained by taking integration on u twice.

Considering numerical simulation and hardware implementation where we need to discretize our model spatially along the backbone curve, it seems reasonable to model a hyper-flexible system with one-dimensional structure as a finite serial-rigid chain from the beginning. Actually, Hashimoto et al. modeled a string as a finite serial-rigid chain in string manipulation (Ichikawa and Hashimoto, 2001). One of the benefit of our exact continuum modeling of a hyper-flexible system is the affinity with spatial geometry. For example, θ in (1), which is one of the most important variables in this dynamics representation, is exactly the curvature of the backbone curve of the flexible object. Therefore, we can understand the values and equations appeared in the kinematics, dynamics and control geometrically, which will help us to build up a user-friendly and flexible manipulation theory. We have already derived the geometric interpretations of the inertia component $\mathcal{M}$ and Γ which defines the Coriolis component. See (Mochiyama and Suzuki, 2002) for more details about the geometric interpretations.

In the same manner as normal dynamics of a serial-rigid chain, the positive definiteness and the symmetry of the inertial component $\mathcal{M}$ and the skew symmetry of $\mathcal{M}_t - 2\mathcal{C}$ hold for this hyper-flexible system. See (Mochiyama and Suzuki, 2003*b*) for the proofs.

3. PASSIVITY-BASED CONTROL

In this paper, the control objective is to suppress the oscillation of a cable-like hyper-flexible body by the translational acceleration input at the one end of the cable under gravitational influence. We do not care the position of the moving base here.

3.1 Port-controlled Hamiltonian Representation

To achieve passivity-based control, we utilize the port-controlled Hamiltonian representation (van der Schaft, 2000) of the hyper-flexible system as follows:

$$\boldsymbol{x}_t(\sigma,t) = \boldsymbol{J}(\boldsymbol{x}(\sigma,t))\frac{\delta H}{\delta \boldsymbol{x}}(\sigma,t) + \boldsymbol{B}(\boldsymbol{x}(\sigma,t))u, \quad (\sigma \in [0\ l]) \tag{7}$$

where $H(t) \in \Re$ denotes the Hamiltonian of the system, which is defined by the sum of the kinetic energy K and the gravitational potential energy P as follows:

$$H(t) := K(t) + P(t) \tag{8}$$

$$K(t) := \frac{1}{2}\int_0^l \int_0^l \theta_t(\eta,t)\mathcal{M}(\eta,\xi,t)\theta_t(\xi,t)d\eta d\xi$$

$$P(t) := -\int_0^l \tilde{m}(\eta)\cos\phi(\eta,t)d\eta\ g\ .$$

$\boldsymbol{x}(\sigma,t) \in \Re^2$, $\boldsymbol{J}(\boldsymbol{x}(\sigma,t)) \in \Re^{2\times 2}$ and $\boldsymbol{B}(\boldsymbol{x}(\sigma,t)) \in \Re^2$ are given as follows:

$$\boldsymbol{x}(\sigma,t) := \begin{bmatrix} \theta(\sigma,t) \\ \varrho(\sigma,t) \end{bmatrix} \tag{9}$$

$$\boldsymbol{J}(\boldsymbol{x}(\sigma,t)) := \begin{bmatrix} 0 & 1 \\ -1 & 0 \end{bmatrix} \tag{10}$$

$$\boldsymbol{B}(\boldsymbol{x}(\sigma,t)) := \begin{bmatrix} 0 \\ \int_\sigma^l \tilde{m}(\eta)\cos\phi(\eta,t)d\eta \end{bmatrix} \tag{11}$$

where $\varrho(\sigma,t) \in \Re$ means the kinetic momentum of the hyper-flexible system at σ defined by

$$\varrho(\sigma,t) := \int_0^l \mathcal{M}(\sigma,\xi,t)\theta_t(\xi,t)d\xi \tag{12}$$

3.2 Passivity

The system output energetically dual with the input u, $y \in \Re$ is

$$y = \int_0^l \frac{\delta H}{\delta \boldsymbol{x}}^T(\sigma,t)\boldsymbol{B}(\boldsymbol{x}(\sigma,t))d\sigma \tag{13}$$

Then, the time derivative of the Hamiltonian along the trajectory of the system can be calculated as

$$\begin{aligned}\frac{dH}{dt}(t) &= \int_0^l \frac{\delta H}{\delta \boldsymbol{x}}^T(\sigma,t)\boldsymbol{x}_t(\sigma,t)d\sigma \\ &= \int_0^l \frac{\delta H}{\delta \boldsymbol{x}}^T(\sigma,t)\boldsymbol{J}(\boldsymbol{x}(\sigma,t))\frac{\delta H}{\delta \boldsymbol{x}}(\sigma,t) \\ &\quad + \frac{\delta H}{\delta \boldsymbol{x}}^T(\sigma,t)\boldsymbol{B}(\boldsymbol{x}(\sigma,t))ud\sigma \\ &= yu\ ,\end{aligned} \tag{14}$$

which shows that the system is passive from u to y (Khalil, 2002).

Moreover, this system is zero-state detectable as well (Khalil, 2002). See (Mochiyama and Suzuki, 2003*b*) for the proof.

The system output y is the time derivative of the gravitational torque at the fixed end of the cable ($\sigma = 0$) divided by the gravitational acceleration constant g. We can see the above fact by the following calculation:

$$\begin{aligned} y &= \int_0^l \theta_t(\sigma,t)\int_\sigma^l \tilde{m}(\eta)\cos\phi(\eta,t)d\eta d\sigma \\ &= \int_0^l \int_0^\eta \theta_t(\sigma,t)d\sigma\tilde{m}(\eta)\cos\phi(\eta,t)d\eta \\ &= \int_0^l \tilde{m}(\eta)\cos\phi(\eta,t)\phi_t(\eta,t)d\eta \\ &= \frac{\partial}{\partial t}\int_0^l \tilde{m}(\eta)\sin\phi(\eta,t)d\eta \\ &= \frac{1}{g}\mathcal{G}_t(0,t)\end{aligned} \tag{15}$$

The system output y is also related to the mass center of the cable $\boldsymbol{p}_{\mathrm{COM}}(t)$. This value can be represented by

$$\boldsymbol{p}_{\mathrm{COM}}(t) = \frac{1}{M}\int_0^l m(\eta)\boldsymbol{p}(\eta,t)d\eta$$

$$= \frac{1}{M} \int_0^l \tilde{m}(\eta) \begin{bmatrix} \cos\phi(\eta,t) \\ \sin\phi(\eta,t) \\ 0 \end{bmatrix} d\eta \quad (16)$$

where M is the total mass of the cable, $\boldsymbol{p}(\sigma, t)$ denotes the position vector between the base origin and the point on the curve at σ viewed from the base coordinate frame. The above expression shows that the system output y is the horizontal component of the time derivative of the mass center of the cable multiplied by the total mass M.

3.3 Damping Injection

For damping injection to the hyper-flexible system, consider the following feedback control law:

$$u = -\psi(y) \quad (17)$$

where $\psi(\cdot)$ is the function satisfying that $\psi(0) = 0$ and $y\psi(y) > 0$ for arbitrary y except zero. By this control law, the time derivative of the Hamiltonian along the trajectory becomes

$$\frac{dH}{dt}(t) = -Ky\psi(y) \leq 0 \quad (18)$$

which shows that dH/dt is negative semi-definite. By the zero-state detectability of the system and applying the infinite-dimensional version of the LaSalle's invariant principle (Michel and Wang, 1994; Luo *et al.*, 1999), we expect that $\boldsymbol{x}(\sigma, t) \to \mathbf{0}$.

For the rigorous proof of the asymptotic stability of the system, we need to properly select the functional space in which the system is represented.

4. SIMULATION

For numerical simulations of the hyper-flexible system, it is necessary to discretize the system not only in time, but also in space along the backbone of the cable i.e., discretization with respect to σ. In this study, we use a planar serial-rigid chain with sufficiently many degrees of freedom as the discretized model of the continuum hyper-flexible cable.

4.1 Computational conditions

The planar serial-rigid chain used in this simulation consists of the moving base, identical 50 rigid bodies, and 50 one-degree-of-freedom rotational joints which connect the base and the links in series. The rigid bodies are identical in shape and mass distribution. The total mass and length of the cable, M and L, are of 1.0 [kg] and 1.0[m] respectively. The mass of the moving base M_B is of 34.4[kg]. We ignore the mass of the joints.

The space sampling is considered to be sufficient because there are 50 joints for a 1.0-meter-long cable, which means that we have a degree of freedom at 0.02 [m] interval along the backbone curve. On the other hand, the sampling time is of 0.001[s].

In the simulation, we have the following equation of motion of the base in the horizontal direction:

$$M_B u = f_B + f_M \quad (19)$$

where f_B denotes the horizontal (y-directional) translational force of the base as the external input and f_M denotes the horizontal inertial force generated by the motion of the cable. In the control design, we ignore this f_M, because this is negligible due to small mass of the cable compared with the force exerted to the base. For small f_M, the external input in the simulation f_B is proportional to the input in the control design u. Of course, in the simulation we take f_M into account rigorously to show that our simplification is reasonable.

In the initial condition, the hyper-flexible cable remains stationary on a straight line downward, i.e., $\boldsymbol{x}_t(\sigma, 0) = \mathbf{0}, \forall\sigma \in [0\ l]$. Then, we apply the following disturbance input to the cable during the first 2 seconds:

$$f_B = \begin{cases} 0 & (0 \leq t < 0.5) \\ 100 & (0.5 \leq t < 1.0) \\ -100 & (1.0 \leq t < 1.5) \\ 0 & (1.5 \leq t < 2.0) \end{cases} \quad (20)$$

Fig. 2 shows the time graph of the input to the cable (upper) and of the gravitational potential energy of the cable P for the free motion i.e., no control after the time 2[s]. We can see the periodic response of the potential energy by the initial disturbance force.

4.2 Control

As shown in the previous section, the system output y is the horizontal component of the time derivative of the mass center of the cable multiplied by the total mass M. Then, in this simulation where the discretized 50 dofs serial-rigid chain model is used instead, we consider the following value $\tilde{y}$ instead of the system output:

$$\tilde{y} = M \frac{d}{dt} \left(\boldsymbol{e}_{\mathrm{y}}^T \frac{\sum_1^{50} m\, \boldsymbol{p}_{\mathrm{COM},i}}{M} \right)$$

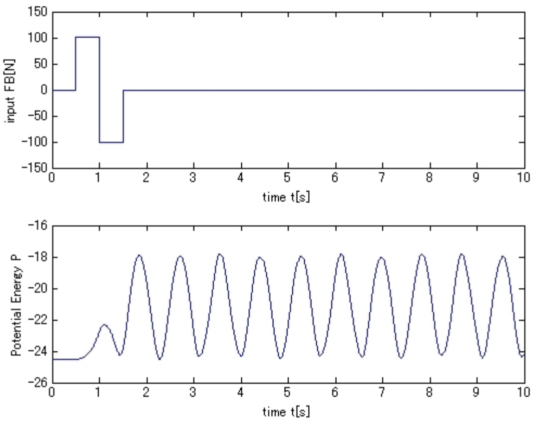

Fig. 2. Input signal (upper) and control-free response of the potential energy (lower)

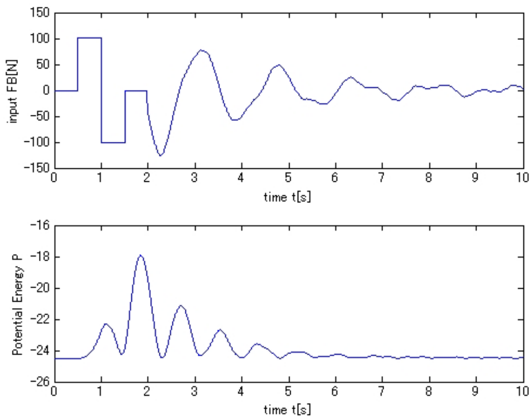

Fig. 3. Input signal (upper) and response of the potential energy (lower) in passivity-based damping control

$$= \frac{1}{50}\frac{d}{dt}\left(\sum_{i=1}^{50} \boldsymbol{e}_{\mathrm{y}}^T \boldsymbol{p}_{\mathrm{COM},i}\right) \qquad (21)$$

where $\boldsymbol{p}_{\mathrm{COM},i} \in \Re^3$ is the position vector of the center of mass of the i-th rigid body, and $m = 0.02$[kg] stands for the mass of the link. Here we consider the following control law:

$$u = -kM_B\tilde{y} \qquad (22)$$

or equivalently

$$f_B = -k\tilde{y} \qquad (23)$$

where k is a positive constant. In this simulation, the value of k is set as 100.0.

The lower graph of Fig. 3 shows the time response of the gravitational potential energy P when we apply the control law (22) after the time 2[s]. In the same manner as Fig. 2, the upper time graph shows the horizontal input force to the cable. We can see the effective damping injection to the cable by the control.

5. CONCLUSION

In this paper, we showed an illustrative control example of dynamics manipulation of hyper-flexible bodies. The authors believe that this simple example is useful to connect real robot systems and rigorous mathematical control theory to build up a useful robotic manipulation theory. The next step is to realize this phenomenon using a real robotic system.

REFERENCES

Arisumi, H., T. Kotoku and K. Komoriya (1999). Swing motion control of casting manipulation. *IEEE Control Systems* **19-4**, 56–64.

Ichikawa, T. and M. Hashimoto (2001). Dynamic manipulation of a string by a robot manipulator (in japanese). *Proc. of the 19th Annual Conference of Robotics Society of Japan* pp. 1243–1244.

Khalil, H.K. (2002). *Nonlinear Systems, 3rd ed.*. Prentice Hall.

Kobayashi, S. (1995). *Differential Geometry of Curves and Surfaces (in Japanese)*. Shokabo. Tokyo.

Luo, Z.H., B.Z. Guo and O. Morgul (1999). *Stability and Stabilization of Infinite Dimensional Systems with Applications*. Springer.

Michel, A.N. and K. Wang (1994). *Qualitative Theory of Dynamical Systems, The Role of Stability Preserving Mappings*. Marcel Dekker.

Mochiyama, H. and T. Suzuki (2002). Geometry of planar hyper-flexible manipulator dynamics (in japanese). *Proc. of the 20th Annual Conference of the Robotics Society of Japan* pp. 3E34(1)–(4).

Mochiyama, H. and T. Suzuki (2003*a*). Kinematics and dynamics of a cable-like hyper-flexible manipulator. *Proc. of the IEEE International Conference on Robotics and Automation* pp. 3672–3677.

Mochiyama, H. and T. Suzuki (2003*b*). Passivity-based damping control of a hyper-flexible manipulator (in japanese). *Proc. of the 8th Robotics Symposia*.

van der Schaft, A.J. (2000). *L_2-Gain and Passivity Techniques in Nonlinear Control.* Springer.

Wakamatsu, H., A. Tsumaya, E. Arai and S. Hirai (2004). Planning of one-handded knotting/raveling manipulation of linear ojbects. *Proc. of the IEEE International Conference on Robotics and Automation* pp. 1719–1725.